

Code-Aided Channel Estimation in LDPC-Coded MIMO Systems

Binghui Shi, Yongpeng Wu, *Senior Member, IEEE*, Peihong Yuan, *Member, IEEE*,
Derrick Wing Kwan Ng, *Fellow, IEEE*, Xiang-Gen Xia *Fellow, IEEE*, and Wenjun Zhang, *Fellow, IEEE*

Abstract—For a multiple-input multiple-output (MIMO) system with unknown channel state information (CSI), a novel low-density parity check (LDPC)-coded transmission (LCT) scheme with joint pilot and data channel estimation is proposed. To fine-tune the CSI, a method based on the constraints introduced by the coded data from an LDPC code is designed such that the MIMO detector exploits the fine-tuned CSI. For reducing the computational burden, a coordinate ascent algorithm is employed along with several approximation methods, effectively reducing the required times of MIMO detection and computational complexity to achieve a satisfying performance. Simulation results utilizing WiMAX standard LDPC codes and quadrature phase-shift keying (QPSK) modulation demonstrate gains of up to 1.3 dB at a frame error rate (FER) of 10^{-4} compared to pilot-assisted transmission (PAT) over Rayleigh block-fading channels.

Index Terms—LDPC codes, fading channel, multiple-input multiple-output (MIMO) system, channel estimation, pilot-assisted transmission (PAT).

I. INTRODUCTION

Multiple-input multiple-output (MIMO) has been widely adopted to enhance data rates and reduce error probabilities in wireless systems [1], [2]. The accurate knowledge of channel state information (CSI) is crucial for achieving efficient communication for a MIMO system. In practical scenarios, pilot symbols are commonly incorporated to estimate the CSI and the estimated CSI is treated as the actual one at the receiver. This technique is known as pilot-assisted transmission (PAT) [3] with mismatched decoding [4].

For short block lengths, PAT with mismatched decoding tends to exhibit sub-optimal performance due to the trade-off between the accuracy of CSI and code rate [5], [6]. Indeed, PAT estimates CSI only based on the pilot symbols, and neglects the inherent channel information embedded in the data symbols. Inspired by this idea, several signal processing methods have been proposed to aid channel estimation [7]–[15]. These methods are mainly based on two principles. First, received symbols are drawn from input alphabet with known distribution. Second, received signals are derived from the known codebook of the channel coding.

Based on the first principle, iterative channel estimation and data detection was proposed [8], [9], which treats the detected symbols as pilots. Furthermore, iterative channel estimation and decoding was proposed [10], [11], where the soft information from decoder is utilized to obtain more accurate distribution of every symbol in the input alphabet. Besides, another effective strategy, termed data-aided channel estimation [12]–[14], has been designed which allows the receiver to exploit partial data symbols as additional pilot symbols for acquiring a more accurate CSI.

Based on the second principle, polar codes with successive cancellation list (SCL) decoding was exploited to estimate CSI for a single-input single-output (SISO) system [15]. In particular, SCL decoding of polar codes is able to provide soft estimation of frozen bits, which can evaluate the probability that the received signals originate from the codebook.

In this work, we propose a scheme realizing code-aided channel estimation for low-density parity-check (LDPC) coded systems based on the second principle. The parity checks of a LDPC code are efficient to measure the probability of “the received sequence is a noisy observation of a codeword”, so they are applied to improve the quality of channel estimation. Furthermore, the coordinate ascent algorithm and a log-likelihood ratio (LLR) approximation method are proposed such that the scheme is adoptable to MIMO systems. We denote this scheme as LDPC-coded transmission (LCT). We obtain a performance gain of up to 1.3 dB at a frame error rate (FER) of 10^{-4} compared to classic PAT schemes exploiting the same number of pilot symbols. LCT also performs close to the FER of the scheme with perfect CSI. LCT also benefits for demodulation reference signal (DMRS) patterns which only have one DMRS symbol in each subcarrier in practical 5G systems.

This paper is organized as follows. Sec. II introduces the notation and background. Sec. III describes our code-aided channel estimation algorithm. Sec. IV shows the numerical results of the proposed method for short LDPC codes under different conditions. Sec. V concludes the paper.

II. PRELIMINARIES

Uppercase letters, e.g., X , denote random variables while lowercase letters, e.g., x , denote their realizations. The probability distribution of X evaluated at x is written as $P_X(x)$. Lower case boldface letters, e.g., \mathbf{x} , denote column vectors. Capital boldface letters, e.g., \mathbf{X} , denote matrices and capital boldface letters with a bar over them, e.g., $\bar{\mathbf{X}}$, denote random matrices. Let $\mathbf{0}_{m \times n}$ be the all zero matrix and $\mathbf{E}_{i,j}$ be the matrix whose element on the i th row and j th column is 1

B. Shi, Y. Wu, and W. Zhang are with the Department of Electronic Engineering, Shanghai Jiao Tong University, Minhang 200240, China (e-mail: zepo@sjtu.edu.cn; yongpeng.wu@sjtu.edu.cn; zhangwenjun@sjtu.edu.cn) (Corresponding author: Yongpeng Wu).

P. Yuan is with the Research Laboratory of Electronics, Massachusetts Institute of Technology, Cambridge, MA, USA (email: phyuan@mit.edu).

D. W. K. Ng is with the School of Electrical Engineering and Telecommunications, University of New South Wales, Sydney, NSW, Australia (e-mail: w.k.ng@unsw.edu.au).

X.-G. Xia is with the Department of Electrical and Computer Engineering, University of Delaware, Newark, DE 19716, USA. (e-mail: xxia@ee.udel.edu).

and all the other elements are 0. We represent $\|\cdot\|$ for the l_2 -norm and $\|\cdot\|_F$ for the Frobenius norm. Let \oplus denote the exclusive OR operation, \mathbb{C} denote the complex field, \Re denote the real part of a complex number and $(\cdot)^H$ denote the conjugate transpose.

A. System Model

Consider a point-to-point MIMO system with N_t transmit antennas and N_r receive antennas. We assume that the fading coefficients in \mathbf{H} are constant during n channel uses. Let \mathcal{X} denote the input alphabet and the channel output is

$$\mathbf{Y} = \mathbf{H}\mathbf{X} + \mathbf{Z},$$

where $\mathbf{X} \in \mathcal{X}^{N_t \times n}$ and $\mathbf{Y} \in \mathbb{C}^{N_r \times n}$ are the transmitted and received signal matrices, $\mathbf{H} \in \mathbb{C}^{N_r \times N_t}$ is the fading channel matrix, and $\mathbf{Z} \in \mathbb{C}^{N_r \times n}$ is additive white Gaussian noise (AWGN) matrix whose entries follow independent and identically distributed (i.i.d.) complex Gaussian distribution with zero-mean and variance $2\sigma^2$, i.e., $\mathcal{CN}(0, 2\sigma^2)$. Neither the transmitter nor the receiver knows the value of \mathbf{H} or its probability distribution $\tilde{\mathbf{H}}$. We assume that the noise variance $2\sigma^2$ is known to the receiver by long term measurement.

Consider the use of quadrature phase-shift keying (QPSK) and 16-quadrature amplitude modulation (QAM) with Gray labeling. The input alphabet is $\mathcal{X} = \frac{1}{\sqrt{2}}\{\pm 1 \pm j\}$ for QPSK and $\mathcal{X} = \frac{1}{\sqrt{10}}\{\pm a \pm jb | a, b \in \{1, 3\}\}$ for 16-QAM. We map a binary vector $\mathbf{c} \in \{0, 1\}^{nN_t k}$ to $\mathbf{X} \in \mathcal{X}^{N_t \times n}$ through the modulator with $k = 2$ for QPSK and $k = 4$ for 16-QAM. A random interleaver permutes the encoded bits \mathbf{c} right before the modulator. We assume that all the symbols in \mathcal{X} are equally probable.

B. LDPC Codes

An LDPC code of rate $r = K/N$ is defined by its parity check matrix H of size $(N - K) \times N$ whose elements are binary, which encodes the information bits $\{u_i\}_{i=1}^K$ to codeword $\{c_i\}_{i=1}^N$. Each row of the parity check matrix H represents a constraint on the encoded message \mathbf{c} . The constraint of the i th row is

$$\bigoplus_{j=1}^{n_i} c_{k_{i,j}} = 0, \quad i = 1, \dots, N - K,$$

where n_i represents the number of ones in the i th row of the parity check matrix H and $k_{i,j}$ represents the position of the j th one in the i th row. Let $W = \max_{i=1, \dots, M} n_i$ represent the maximum number of ones in all the rows. For ease of presentation, we denote $N - K$ as M in the following.

The parity check matrix H has a significant impact on the performance of an LDPC code, so the selection of H is specified in numerous standards. In this work, LDPC codes from WiMAX in IEEE 802.16 are adopted.

The belief propagation (BP) decoder iteratively computes the probability p_i that the bit c_i in \mathbf{c} equals 1 when all the constraints are satisfied. The iteration count R of the BP decoder refers to the maximum iteration number in case the parity check matrix H cannot be satisfied.

C. Pilot-Assisted Transmission

In PAT, the first n_p symbols are pilot symbols \mathbf{X}_p and the remaining $n_d = n - n_p$ symbols \mathbf{X}_d are coded. The pilot and coded symbols have the same amount of energy, and the pilot symbols are known to the receiver. The received signals of \mathbf{X}_p and \mathbf{X}_d are denoted as \mathbf{Y}_p and \mathbf{Y}_d , respectively. We set $N = n_d N_t k$ to keep the block length fixed. In this paper with PAT, a linear minimum mean square error (LMMSE) channel estimator is adopted to obtain CSI with the received signal \mathbf{Y}_p . The LMMSE estimator is [16]

$$\hat{\mathbf{H}} = \mathbf{Y}_p \mathbf{X}_p^H (\mathbf{X}_p \mathbf{X}_p^H + 2\sigma^2 \mathbf{I}_{N_t})^{-1}.$$

We adopt a bit-interleaved coded modulation (BICM) [17] encoder at the transmitter and a bit-metric decoder at the receiver. With given $\mathbf{Y}_d, \hat{\mathbf{H}}$, a maximum-likelihood (ML) detector with log-sum approximation is applied to obtain the bit-wise LLRs. Let $L_i, i = 1, \dots, N$, denote the LLRs of every bit, then for $i = 1, \dots, N$,

$$L_i = \frac{1}{2\sigma^2} \left(\min_{\mathbf{x} \in Q_i^1} \|\mathbf{y}_i - \hat{\mathbf{H}}\mathbf{x}\|^2 - \min_{\mathbf{x} \in Q_i^0} \|\mathbf{y}_i - \hat{\mathbf{H}}\mathbf{x}\|^2 \right), \quad (1)$$

where $\mathbf{y}_i \in \mathbb{C}^{N_r}$ is the column of \mathbf{Y}_d which contains c_i and $Q_i^0 \subset \mathcal{X}^{N_t}$ contains all the vectors whose $c_i = 0$, $Q_i^1 \subset \mathcal{X}^{N_t}$ contains all the vectors whose $c_i = 1$.

III. CODE-AIDED CHANNEL ESTIMATION

This section presents a code-aided channel estimation scheme for an LDPC-coded MIMO system. Through this scheme, we can fine-tune the channel estimation and achieve a better FER performance.

Let binary random variables $\{Z_i\}_{i=1}^M$ denote whether the constraint of the i th row of the parity check matrix H is satisfied, and $z_i = 0$ indicates that the constraint of the i th row is satisfied. Let binary random variables $\{\Pi_i\}_{i=1}^M$ denote whether the constraints of the first i rows of the parity check matrix H are satisfied and $\Pi_i = 0$ indicates that they are satisfied. For notation consistency, let Π_0 denote a binary random variable that $P_{\Pi_0}(0) = 1$ and is uncorrelated to Z_i .

Since the parity check matrix H of an LDPC code is sparse, the probability that the received sequence is a codeword can be accurately approximated by the probability that all the constraints of LDPC code are satisfied. Then, we calculate this probability with the given $\hat{\mathbf{H}}$ to fine-tune the channel estimation as

$$\begin{aligned} \mathbf{H}^* &= \arg \max_{\hat{\mathbf{H}}} P_{\Pi_M | \bar{\mathbf{Y}}_d, \bar{\mathbf{H}}} (0 | \mathbf{Y}_d, \hat{\mathbf{H}}) \\ &= \arg \max_{\hat{\mathbf{H}}} \prod_{i=1}^M P_{Z_{M-i+1} | \Pi_{M-i}, \bar{\mathbf{Y}}_d, \bar{\mathbf{H}}} (0 | \mathbf{Y}_d, \hat{\mathbf{H}}). \end{aligned} \quad (2)$$

A. Channel Estimation Fine-tuning

With the fixed $\mathbf{Y}_d, \hat{\mathbf{H}}$, we first calculate the LLR of every bit by the ML detector (1). For simplicity, we ignore $\mathbf{Y}_d, \hat{\mathbf{H}}$ in the following equations.

Let $\{C_i\}_{i=1}^N$ be the binary random variables representing every received bit and $\{c_i\}_{i=1}^N$ are their realizations. Then, for $i = 1, 2, \dots, M$, we have

$$P_{Z_i}(0) = P\left(\bigoplus_{j=1}^{n_i} c_{k_{i,j}} = 0\right) \quad (3)$$

$$= \frac{1}{2} + \frac{1}{2} \prod_{j=1}^{n_i} \left(1 - 2P_{C_{k_{i,j}}}(1)\right).$$

If all the rows of parity check matrix are uncorrelated, then every term in (2) is

$$P_{Z_{M-i+1}|\Pi_{M-i}}(0|0) = P_{Z_{M-i+1}}(0) \quad (4)$$

and R.H.S of (4) is obtained by (3).

However, since the rows with a 1 in the same column are correlated, (4) does not always hold. According to the algorithm of BP decoder, every term of the product in (2) is approximated as follows.

Let $L_{X|Y} = \ln\left(\frac{P_{X|Y}(x=0|y=0)}{P_{X|Y}(x=1|y=0)}\right)$ represent the LLR of x given $y = 0$ and $L_X = \ln\left(\frac{P(x=0)}{P(x=1)}\right)$ represent the LLR of x . Then, convert (3) into LLR form that yields

$$L_{Z_i|\Pi_{i-1}} = 2 \tanh^{-1} \left(\prod_{j=1}^{n_i} \left(\tanh \left(\frac{L_{C_{k_{i,j}}|\Pi_{i-1}}}{2} \right) \right) \right), \quad (5)$$

where $p_{C_j|\Pi_i}(1|0)$ in $L_{C_j|\Pi_i}$ is updated by the following steps and $L_{C_j|\Pi_0} = L_j$ are the LLRs computed by the $\mathbf{Y}_d, \hat{\mathbf{H}}$. For $j = 1, 2, \dots, N$, we have

$$P_{C_j|\Pi_i}(0|0) = \frac{P_{Z_i|C_j,\Pi_{i-1}}(0|0,0)}{P_{Z_i|\Pi_{i-1}}(0|0)} P_{C_j|\Pi_{i-1}}(0|0), \quad (6)$$

where if $j \in \{k_{i,m} | m = 1, \dots, n_i\}$,

$$P_{Z_i|C_j,\Pi_{i-1}}(0|0,0) = \frac{1}{2} + \frac{1}{2} \prod_{m=1, k_{i,m} \neq j}^{n_i} \left(1 - 2P_{C_{k_{i,m}}|\Pi_{i-1}}(1|0)\right),$$

else

$$P_{Z_i|C_j,\Pi_{i-1}}(0|0,0) = P_{Z_i|\Pi_{i-1}}(0|0).$$

We convert (6) to LLR form and obtain if $j \in \{k_{i,m} | m = 1, \dots, n_i\}$,

$$L_{C_j|\Pi_i} = 2 \tanh^{-1} \left(\prod_{m=1, k_{i,m} \neq j}^{n_i} \left(\tanh \left(\frac{L_{C_{k_{i,m}}|\Pi_{i-1}}}{2} \right) \right) \right) + L_{C_j|\Pi_{i-1}}. \quad (7)$$

Also, we convert $p_{\Pi_i} = p_{Z_i|\Pi_{i-1}} p_{\Pi_{i-1}}$ to LLR form and have

$$L_{\Pi_i} = L_{Z_i|\Pi_{i-1}} + L_{\Pi_{i-1}} - \log \left(1 + e^{L_{Z_i|\Pi_{i-1}}} + e^{L_{\Pi_{i-1}}} \right). \quad (8)$$

The algorithm to calculate $P_{\Pi_M}(0)$ in LLR form is summarized in Algorithm 1.

The computational complexity of calculating L_{Π_M} given $\mathbf{Y}_d, \hat{\mathbf{H}}$ is $\mathcal{O}(MW)$, which is the same as one round of the BP decoder. We denote Algorithm 1 without updating $L_{C_j|\Pi_i}$ via (7) in line 3 as Algorithm 1a. The comparison between Algorithm 1 and Algorithm 1a is given in Section IV.

Algorithm 1 Metric Calculation Algorithm

Input: the LLRs of every bit $\{L_i\}_{i=1}^N$, parity check matrix H

- 1: **for** $i = 1$ to M **do**
- 2: calculate $L_{Z_i|\Pi_{i-1}}$ via (5)
- 3: update $L_{C_j|\Pi_i}$ via (7)
- 4: combine $L_{Z_i|\Pi_{i-1}}$ and $L_{\Pi_{i-1}}$ via (8) and get L_{Π_i}
- 5: **end for**

Output: L_{Π_M} , which is $P_{\Pi_M}(0)$ in LLR form

B. Coordinate Ascent Algorithm

A direct method to solve (2) is via an exhausting search. However, the search space in (2) grows exponentially in terms of $N_r N_t$. As a compromise approach, we adopt a coordinate ascent method to acquire a high-quality solution. A channel estimation $\hat{\mathbf{H}}$ is firstly obtained by LMMSE. In the coordinate ascent, every element of $\hat{\mathbf{H}}$ is optimized one-by-one. When optimizing one element, its real and imaginary parts are optimized sequentially. When optimizing one part, we adopt a grid search to find the maximum point in a fixed neighborhood with the other elements fixed. Algorithm 2 specifies the overall process.

Algorithm 2 Code-Aided Channel Estimation Algorithm

Input: the received vector \mathbf{y} , parity check matrix H , the LMMSE channel estimation result $\hat{\mathbf{H}}$

- 1: $\tilde{\mathbf{H}} \leftarrow \hat{\mathbf{H}}$, $\tilde{\mathbf{H}}$ is the code-aided channel estimation
- 2: **repeat**
- 3: $\Delta \mathbf{H} \leftarrow \mathbf{0}_{N_r \times N_t}$
- 4: obtain the LLRs of every bit given $\tilde{\mathbf{H}}$ via (1)
- 5: **for** $i = 1$ to N_r **do**
- 6: **for** $j = 1$ to N_t **do**
- 7: obtain the LLRs of every bit given $\Delta \mathbf{H}, h$ via (9)
- 8: obtain $L_{\Pi_M}(h)$ via Algorithm 1
- 9: find $h_{\max} = \arg \max_h L_{\Pi_M}(h)$
- 10: $\Delta \mathbf{H} \leftarrow \Delta \mathbf{H} + h_{\max} \mathbf{E}_{i,j}$ and update p_i and q_i
- 11: **end for**
- 12: **end for**
- 13: $\tilde{\mathbf{H}} \leftarrow \tilde{\mathbf{H}} + \Delta \mathbf{H}$
- 14: **until** $\|\Delta \mathbf{H}\|_F \leq \varepsilon$

Output: the code-aided channel estimation $\tilde{\mathbf{H}}$

When optimizing the element at the r th row and c th column of $\tilde{\mathbf{H}}$, we first set

$$\Delta \mathbf{H}'(h) = \Delta \mathbf{H} + h \mathbf{E}_{r,c}$$

and then get the LLRs of every bit by \mathbf{y}, \mathbf{H}' . The value of $h \in \mathbb{C}$ is enumerated to maximize L_{Π_M} . The step size is set to $b\sigma^2/n_p$ where b is a parameter to balance the accuracy and computational complexity. The reason using this step size is that $\|\hat{\mathbf{H}} - \mathbf{H}\|_F^2$ is approximately proportional to σ^2/n_p .

We assume that $\|\hat{\mathbf{H}} - \tilde{\mathbf{H}}\|_F$ is small. So the value of $\|\Delta \mathbf{H}\|_F$ is small in every iteration. Therefore, we assume that for $i = 1, 2, \dots, N$,

$$\mathbf{x}_i^1 = \arg \min_{\mathbf{x} \in Q_i^1} \|\mathbf{y} - \tilde{\mathbf{H}} \mathbf{x}\|^2, \quad \mathbf{x}_i^0 = \arg \min_{\mathbf{x} \in Q_i^0} \|\mathbf{y} - \tilde{\mathbf{H}} \mathbf{x}\|^2$$

in (1) are the same as the ones when $\tilde{\mathbf{H}}$ replaced by $\mathbf{H}' = \tilde{\mathbf{H}} + \Delta\mathbf{H}'$.

With given h and $\{L_i\}_{i=1}^N$ under $\tilde{\mathbf{H}} + \Delta\mathbf{H}$, the LLRs under $\tilde{\mathbf{H}} + \Delta\mathbf{H}'(h)$ is approximated as

$$\begin{aligned} L'_i &\approx L_i + \frac{1}{\sigma^2} \Re(p_i^H h \mathbf{E}_{r,c} \mathbf{x}_i^0 - q_i^H h \mathbf{E}_{r,c} \mathbf{x}_i^1) \\ &\quad - \frac{1}{2\sigma^2} (\|h \mathbf{E}_{r,c} \mathbf{x}_i^0\|^2 - \|h \mathbf{E}_{r,c} \mathbf{x}_i^1\|^2) \\ &= L_i + \frac{1}{\sigma^2} \Re(h(p_{i,r}^H x_{i,c}^0 - q_{i,r}^H x_{i,c}^1)) \\ &\quad - \frac{|h|^2}{2\sigma^2} (|x_{i,c}^0|^2 - |x_{i,c}^1|^2), \end{aligned} \quad (9)$$

where $p_i = \mathbf{y}_i - (\tilde{\mathbf{H}} + \Delta\mathbf{H})\mathbf{x}_i^0$ and $q_i = \mathbf{y}_i - (\tilde{\mathbf{H}} + \Delta\mathbf{H})\mathbf{x}_i^1$. The values of \mathbf{x}_i^0 and \mathbf{x}_i^1 are stored when executing the ML detector to acquire LLRs under $\tilde{\mathbf{H}}$. The values of p_i and q_i are updated for any h with complexity $\mathcal{O}(N)$ since $h\mathbf{E}_{r,c}$ has only one nonzero element. Without this approximation, we have to execute MIMO detection every time we calculate L_{Π_M} . Now we only need to execute once in every iteration.

Let $L_{\Pi_M,0}$ denote the value of L_{Π_M} under $\tilde{\mathbf{H}} + \Delta\mathbf{H}$, $L_{\Pi_M,0}(h)$ denote the value of L_{Π_M} under $\tilde{\mathbf{H}} + \Delta\mathbf{H}'(h)$, $L_{\Pi_M,1}$ denote the value of L_{Π_M} under $\tilde{\mathbf{H}} + \Delta\mathbf{H}(h_{max})$. Notice that $L_{\Pi_M,0}(0) = L_{\Pi_M,0}$, so $L_{\Pi_M,1} \geq L_{\Pi_M,0}$. Therefore, L_{Π_M} is non-decreasing during iteration. In addition, let

$$P_1 = \max_{\hat{\mathbf{H}}} P_{Z_1|\hat{\mathbf{Y}}_d, \hat{\mathbf{H}}}(0|\mathbf{Y}_d, \hat{\mathbf{H}})$$

and we have

$$P_{\Pi_M}(0) < P_{Z_1|\hat{\mathbf{Y}}_d, \hat{\mathbf{H}}}(0|\mathbf{Y}_d, \mathbf{H}^*) \leq P_1$$

from (2) and $P_1 < 1$ from its definition. So, L_{Π_M} has an upper bound $\ln(P_1/(1 - P_1))$. Based on these two points, The iteration in Algorithm 2 converges. Indeed, the Algorithm 2 converges to a local maximum of (2).

The computational complexity of the coordinate ascent algorithm can be expressed as $\mathcal{O}(N_1(N_2^{kN_t} + NN_tN_r + N_2MW))$, where N_1 is the average iteration count of Algorithm 2 and N_2 is the average number of executing Algorithm 1 in line 8 of Algorithm 2. The first term of the computational complexity pertains to the MIMO detection, the second term is for the updates of p_i and q_i and the third term is the number of times Algorithm 1 is executed. Through simulation, we find that satisfying performance is achieved with limited N_1 (< 10). Therefore, the complexity of Algorithm 2 is acceptable. Furthermore, this complexity can be reduce via MIMO detection with lower complexity, e.g., sphere decoding [18].

Once the code-aided channel estimation $\tilde{\mathbf{H}}$ is obtained, we execute the BP decoder to obtain the decoded word $\hat{\mathbf{u}}$.

IV. NUMERICAL RESULTS

In this section, we provide Monte Carlo simulation results and compare the performance of PAT and LCT. The SNR is expressed as $E_s N_t / (2\sigma^2 N_r)$, where E_s is the energy per symbol. FER is chosen to be the performance criteria. We select the LDPC code in WiMAX with $N = 192$ and $K = 96$. Rayleigh block-fading channel with 2×2 MIMO is considered in all the simulations, e.g., the entries of \mathbf{H} are i.i.d. as

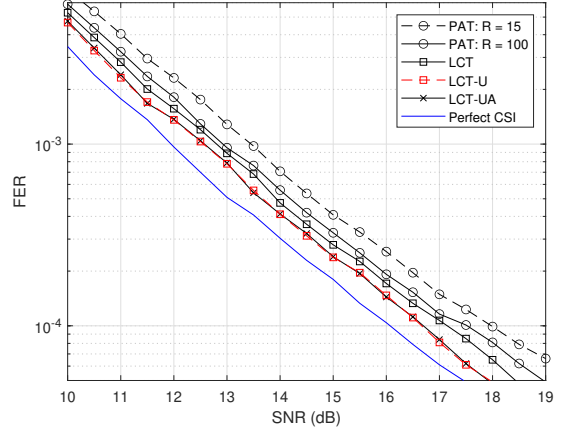


Fig. 1. Performance of PAT and LCT with $\mathbf{H} \in \mathbb{C}^{2 \times 2}$. A (192, 96) LDPC code is adopted with QPSK such that the number n_d of coded symbols is 48. The number n_p of pilot symbols is set to 15.

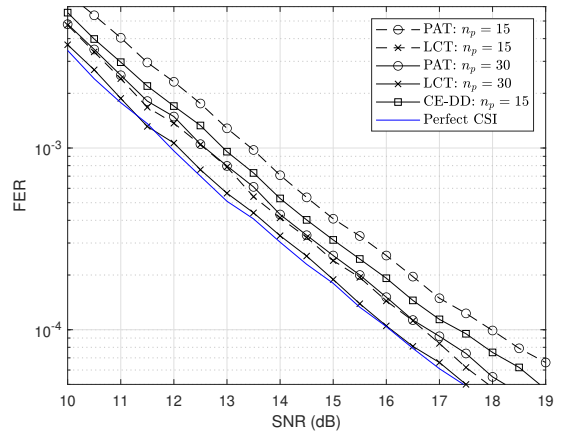


Fig. 2. Performance of PAT and LCT with $\mathbf{H} \in \mathbb{C}^{2 \times 2}$. A (192, 96) LDPC code is adopted with QPSK such that the number n_d of coded symbols is 48. The number n_p of pilot symbols is set to 15 and 30.

$\mathcal{CN}(0, 1)$. The maximum iteration count R is set to 15 in all the simulations unless otherwise indicated. The performance is also compared to a coherent receiver which perfect CSI is available for detection. The Monte Carlo simulation terminates when the number of trials reaches 10^6 or the number of frame errors of coherent receiver with the perfect CSI reaches 200.

A. Performance

This part shows the performance of the two methods. We adopt QPSK and $n_p = 15$ for all conditions. The FERs of different methods are shown in Fig. 1. The iteration count R is additionally set to 100 in PAT to eliminate the influence of insufficient iteration count. LCT refers to Algorithm 2 using (1) to obtain the LLR and Algorithm 1a, LCT-U refers to Algorithm 2 adopting (1) and Algorithm 1, and LCT-UA stands for Algorithm 2 adopting Algorithm 1 and the approximation of LLR in (9).

As shown in Fig. 1, at an FER $\approx 10^{-4}$, the LCT-UA and LCT-U outperform PAT with $R = 100$ by about 0.8 dB and PAT with $R = 15$ by about 1.3 dB. They also perform within 0.6 dB of the receiver with perfect CSI, which proves

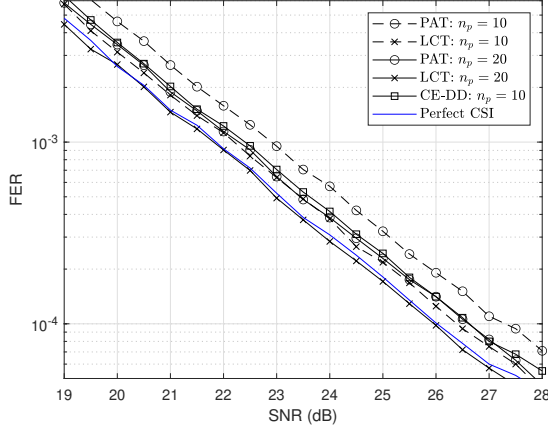


Fig. 3. Performance of PAT and LCT with $\mathbf{H} \in \mathbb{C}^{2 \times 2}$. A (192, 96) LDPC code is used with 16-QAM such that the number n_d of coded symbols is 24. The number n_p of pilot symbols is set to 10 and 20.

TABLE I
THE VALUES OF AVERAGE ITERATION COUNT OF ALGORITHM 2

SNR (dB)	Modulation	N_1	SNR (dB)	Modulation	N_1
10	QPSK	4.36	19	16-QAM	3.15
13	QPSK	5.84	22	16-QAM	3.97
16	QPSK	6.91	25	16-QAM	4.64
19	QPSK	7.69	28	16-QAM	5.08

the effectiveness of LCT. Moreover, the benefit of updating $L_{C_j|\Pi_i}$ via (7) is proven because LCT-U outperforms LCT by about 0.5 dB. We can also find that LCT-UA and LCT-U exhibit identical, which means that the approximation in (9) does not incur any performance penalty. Therefore, we adopt LCT-UA in the following simulations and denote it as LCT.

The gains may originate from a more precise value relation between LLRs of every bit. ML detection with channel estimation $\tilde{\mathbf{H}}$ represents the constrains of LLRs and Algorithm 2 provides the most probable LLRs under these constrains.

B. Impact of n_p

Next, we consider the performance of LCT with different values of n_p to show that the performance gain persists with sufficient pilot symbols. We use QPSK for all the simulations. The values of n_p are 15 and 30. As shown in Fig. 2, the performance of LCT with $n_p = 30$ still outperforms PAT with $n_p = 30$ by about 0.7 dB at an FER $\approx 10^{-4}$. At the same FER, LCT performs within 0.1 dB compared to the receiver with perfect CSI when n_p is 30. The performance of LCT is also compared with CE-DD in [8] for $n_p = 15$. The performance of LCT outperforms CE-DD by about 0.5 dB at an FER $\approx 10^{-4}$ for $n_p = 15$.

C. Higher-order Modulation

We next consider the performance of LCT with 16-QAM under different values of n_p . The values of n_p are 10 and 20. As shown in Fig. 3, the performance of LCT outperforms PAT by about 0.6 dB when $n_p = 10$ and about 0.9 dB when $n_p = 20$ at an FER $\approx 10^{-4}$. At the same FER, the performance of LCT approaches closely that of the receiver with perfect CSI when n_p is 20. The performance of LCT outperforms CE-DD

by about 0.2 dB at an FER $\approx 10^{-4}$ when $n_p = 10$.

The values of N_1 under QPSK and 16-QAM are also given in Table I. The values of n_p for QPSK and 16-QAM are 15 and 10, respectively. We can find that the values of N_1 are not large so the complexity of Algorithm 2 is acceptable.

V. CONCLUSION

Through introducing the parity-check constraints of an LDPC code, an LCT scheme was proposed to fine-tune the estimated CSI in MIMO system. The coordinate ascent algorithm was adopted to handle the exponential growth of solution space. Furthermore, an LLR approximation method was proposed to reduce the times of MIMO detection required by the algorithm. Simulation results showed that LCT outperforms PAT schemes with acceptable complexity.

REFERENCES

- [1] G. Foschini, "Layered space-time architecture for wireless communication in a fading environment when using multi-element antennas," *Bell Labs Tech. J.*, vol. 1, pp. 41–59, 06 2002.
- [2] E. Telatar, "Capacity of multi-antenna Gaussian channels" *Europ. Trans. Telecommun.*, vol. 10, no. 6, pp. 585–595, 1999.
- [3] L. Tong, B. Sadler, and M. Dong, "Pilot-assisted wireless transmissions: General model, design criteria, and signal processing," *IEEE Signal Process. Mag.*, vol. 21, no. 6, pp. 12–25, 2004.
- [4] A. Lapidoth and P. Narayan, "Reliable communication under channel uncertainty," *IEEE Trans. Inf. Theory*, vol. 44, no. 6, pp. 2148–2177, 1998.
- [5] J. Östman, G. Durisi, E. G. Ström, M. C. Coşkun, and G. Liva, "Short packets over block-memoryless fading channels: Pilot-assisted or noncoherent transmission?" *IEEE Trans. Commun.*, vol. 67, no. 2, pp. 1521–1536, 2019.
- [6] G. Taricco and G. Coluccia, "Optimum receiver design for correlated rician fading MIMO channels with pilot-aided detection," *IEEE J. Select. Areas Commun.*, vol. 25, no. 7, pp. 1311–1321, 2007.
- [7] J. Garcia-Frias and J. D. Villaseñor, "Combined turbo detection and decoding for unknown ISI channels," *IEEE Trans. Commun.*, vol. 51, no. 1, pp. 79–85, Jan. 2003.
- [8] C. Cozzo and B. L. Hughes, "Joint channel estimation and data detection in space-time communications," *IEEE Trans. Commun.*, vol. 51, no. 8, pp. 1266–1270, Aug. 2003.
- [9] M. Abuthinien, S. Chen, and L. Hanzo, "Semi-blind joint maximum likelihood channel estimation and data detection for MIMO systems," *IEEE Signal Process. Lett.*, vol. 15, pp. 202–205, Jan. 2008.
- [10] J. Zheng and B. Rao, "LDPC-coded MIMO systems with unknown block fading channels: Soft MIMO detector design, channel estimation, and code optimization," *IEEE Trans. Signal Process.*, vol. 54, no. 4, pp. 1504–1518, 2006.
- [11] C. Herzet, V. Ramon, and L. Vandendorpe, "A theoretical framework for iterative synchronization based on the sum-product and the expectation-maximization algorithms," *IEEE Trans. Signal Process.*, vol. 55, no. 5, pp. 1644–1658, 2007.
- [12] T.-K. Kim, Y.-S. Jeon, J. Li, N. Tavangaran, and H. V. Poor, "Semi-data-aided channel estimation for MIMO systems via reinforcement learning," *IEEE Trans. Wireless Commun.*, vol. 22, no. 7, pp. 4565–4579, 2023.
- [13] P. Singh, H. B. Mishra, A. K. Jagannatham, and K. Vasudevan, "Semi-blind, training, and data-aided channel estimation schemes for MIMO-FBMC-OQAM systems," *IEEE Trans. Signal Process.*, vol. 67, no. 18, pp. 4668–4682, 2019.
- [14] J. Ma and L. Ping, "Data-aided channel estimation in large antenna systems," *IEEE Trans. Signal Process.*, vol. 62, no. 12, pp. 3111–3124, 2014.
- [15] P. Yuan, M. C. Coskun, and G. Kramer, "Polar-coded non-coherent communication," *IEEE Commun. Lett.*, vol. 25, no. 6, pp. 1786–1790, 2021.
- [16] B. Hassibi and B. Hochwald, "How much training is needed in multiple-antenna wireless links?" *IEEE Trans. Inf. Theory*, vol. 49, no. 4, pp. 951–963, 2003.
- [17] G. Caire, G. Taricco, and E. Biglieri, "Bit-interleaved coded modulation," *IEEE Trans. Inf. Theory*, vol. 44, no. 3, pp. 927–946, 1998.

- [18] C. Studer, A. Burg, and H. Bolcskei, “Soft-output sphere decoding: Algorithms and VLSI implementation” *IEEE J. Sel. Areas Commun.*, vol. 26, no. 2, pp. 290–300, Feb. 2008.